Periodica Polytechnica
Electrical Engineering
and Computer Science

OnlineFirst (2017) paper 10224
https://doi.org/10.3311/PPee.10224

RESEARCH ARTICLE

Theoretical Limits of Parameter Estimation Based on Quantized Data

Tamás Virosztek[1*], István Kollár†[1]

Received 28 October 2016; accepted after revision 25 May 2017

Abstract

Parameter estimation of band-limited periodic signals (sine and multisine waves) is a very common task in the field of measurement technology and control engineering. In the overwhelming majority of data acquisition and control systems the analog signals of the real world are sampled an quantized using analog-to-digital converters (ADCs). To estimate the parameters of the analog signal and the parameters of the quantizer from the same measurement record is an obvious need in these cases. The parameters of the recorded signal can be used to calculate the response of our system (e.g. signals of the actuators) while the parameters of the quantizer can be used to identify the transfer characteristic of the measurement channel. Maximum likelihood (ML) estimation of the quantizer and analog signal parameters has been developed to perform this task and to provide asymptotically unbiased and efficient estimators for the quantizer and signal parameters. This paper investigates the theoretical limits of this kind of estimation: provides the Cramér-Rao Lower Bound (CRLB) for the covariance of the achieved estimators and compares them to CRLB values obtained using less complex signal and channel models. This article also provides a comparison of the empirical covariance of estimator populations achieved different ways to the CRLB of estimation. The major tendencies are drawn and explanation for them is provided as well.

Keywords

quantization, parameter estimation, sine wave, maximum likelihood, CRLB

[1] Department of Measurement Technology and Information Systems
Faculty of Electrical Engineering and Informatics,
Budapest University of Technology and Economics
H-1117 Budapest, Magyar tudósok körútja 2., Hungary

[*] Corresponding author, e-mail: virosztek@mit.bme.hu

1 Introduction

The aim of this paper is to investigate the theoretical limits and practical properties of quantizer and signal parameter estimation in that case when parameters of the excitation signal and the quantizer has to be estimated from the same measurement record. This kind of estimation is necessary in the following scenarios:

- A band-limited periodic signal has been acquired via analog-to digital conversion. The signal contains harmonic components and additive noise, and the quantization of the signal is non-ideal. However the parameters (DC offset, frequency and the Fourier components) of the signal shall be estimated paying attention to the nonidealities of the measurement channel (the quantizer). The estimated parameters can be used for multiple applications:
  - to determine power quality based on the harmonic content of the voltage signal of a power transmission line
  - to control the frequency of a power transmission network based on accurate estimation of system frequency
  - to qualify an audio amplifier based on the harmonic distortion and the amount of noise at the output

  and naturally other applications may exist.
- The aim is to qualify the analog-to-digital converter using standard quality measures e.g. effective number of bits (ENOB), signal to noise and distortion ratio (SINAD), integral nonlinearity (INL) differential nonlinearity (DNL), etc. These quantities can be calculated based on the parameter estimators using elemental mathematical operations. Owing to the properties of maximum likelihood estimators [1] the quality measures calculated using the ML estimators of the signal and quantizer parameters are the ML estimators of the quality measures. This way applying a sinusoidal excitation - which necessarily contains additive noise and harmonic components depending on the quality of the sine wave generator – and then calculating the ML estimators of the quantizer and excitation signal parameters one can achieve asymptotically unbiased and asymptotically efficient estimators for the quality measures of the quantizer.

Naturally there can be other scenarios when this kind of parameter estimation is required. The model described in Section 2 uses two restrictions:

- **Gaussian noise model.** The additive noise on the analog excitation signal is modelled as Gaussian white noise. The whiteness of the noise is used in the model when samples of noise are assumed to be uncorrelated. Due to experiments performed with real signal generators and ADCs in laboratory [2] the spectral power density function of the noise is smooth enough to make the white noise model lifelike. The other assumption is the Gaussian distribution. According to the experiments mentioned in [2] the Gaussian noise model is lifelike as well, however it is not required to have Gaussian noise on the excitation signal to make this kind of estimation work. The role of the noise model is to punish strictly monotonically the deviation of the reconstructed signal from the measured values, to decrease the likelihood when the model and the measurements move apart. This way any noise model which has symmetrical and piecewise monotonic probability density function can be used for this purpose. However, Gaussian model gives a good approximation of the reality according to laboratory experiments.
- **Noisy sine wave as excitation signal.** The model described in Section 2 uses a noisy sine wave without higher harmonic components. This model is useful when the quantizer is to be qualified and the test is performed using a sinusoidal excitation signal with the lowest possible harmonic distortion. In this case the signal model contains the fundamental harmonic only. However, the model can be extended to handle higher harmonics as it is described in section 7. This extension only increases the parameter space without increasing the theoretical complexity of the estimation problem.

2 Maximum likelihood estimation of ADC and sine wave parameters using Gaussian noise model

For maximum likelihood estimation of ADC testing the following model has been developed [3]. The converter is described with a set of code transition levels. Transition level $T[k]$ is the value of the input voltage, that results code k-1 with probability of 50%, and code k with probability of 50% as well. The N-bit quantizer provides codes from 0 up to 2^N-1, and has 2^N-1 transition levels. The reduced full scale of the converter is the voltage range between $T[1]$ and $T[2^N\text{-}1]$. Voltage values above the highest transition level result code 2^N-1 and voltages below the lowest transition level result code 0. Quantization can be described with a function $q(x)$ where

$$q(x)=\begin{cases} 0, & x<T[1] \\ m, & T[m]<x<T[m+1] \\ 2^N-1, & x>T\left[2^N-1\right] \end{cases} \tag{1}$$

The sinusoidal excitation signal can be described with four parameters:

$$x(t)=A\cos(2\pi ft)+B\sin(2\pi ft)+C \tag{2}$$

where A is the cosine coefficient, B is the sine coefficient, and C denotes the DC component of the signal. The frequency of the sine wave is denoted with f. The electronic noise of the devices and the imperfections of the measurement environment are modeled with additional noise on the excitation signal. The most manifest is to assume Gaussian noise with zero mean and σ standard deviation. Let $n(t)$ denote the realization of the additive noise. In this model the spectrum of the noise is white, so $n(\tau_1)$ and $n(\tau_2)$ are independent if $\tau_1 \neq \tau_2$. This noisy sine wave is quantized and sampled (the sequence is interchangeable), thus the output of the ADC can be described this way:

$$y(k)=q\left(x(t_k)+n(t_k)\right) \tag{3}$$

where t_k denotes the k^{th} sampling time moment (k = 1..M). The parameters of the model to be estimated to be estimated are the following:

- The code transition levels of the quantizer: $T[1]$, $T[2]$, ..., $T[2^N\text{-}1]$
- The cosine coefficient of the sine wave: A
- The sine coefficient of the sine wave: B
- The DC component of the sine wave: C
- The frequency of the sine wave: f
- The standard deviation of noise on the excitation signal: σ

As uniform sampling is assumed (effects of incidental non-ideal sampling are not considered in this model), the frequency of the sine wave can be described using the angular frequency normalized to the sampling frequency:

$$\theta=\omega T_s=2\pi\frac{f}{f_s} \tag{4}$$

where T_s is the sampling time, and f_s denotes the sampling frequency. Thus the parameter vector to be estimated is the following:

$$\mathbf{p}^T=\left[A\ B\ C\ \theta\ \sigma\ T[1]T[2]\ldots T\left[2^N-2\right]T\left[2^N-1\right]\right] \tag{5}$$

To express the likelihood of the parameters, it is necessary introduce a vector of discrete random variables, denoted by Y. Value Y (k) belongs to the kth sample of the measurement record and can achieve 2^N values: it can be any of the output codes of the ADC form 0 to 2^N-1 with a given probability. These probabilities can be described using the error function:

$$\operatorname{erf}(x)=\frac{2}{\sqrt{\pi}}\int_0^x e^{-z^2}\mathrm{d}z \tag{6}$$

$$P\left[Y(k)=0\right]=\frac{1}{2}\left[\operatorname{erf}\left(\frac{T[1]-x(t_k)}{\sigma\sqrt{2}}\right)+1\right] \tag{7}$$

$$P\left[Y(k)=2^N-1\right]=\frac{1}{2}\left[1-\operatorname{erf}\left(\frac{T\left[2^N-1\right]-x(t_k)}{\sigma\sqrt{2}}\right)\right] \quad (8)$$

$$P\left[Y(k)=l\right]=\frac{1}{2}\left[\operatorname{erf}\left(\frac{T[l+1]-x(t_k)}{\sigma\sqrt{2}}\right)+\operatorname{erf}\left(\frac{T[l]-x(t_k)}{\sigma\sqrt{2}}\right)\right] \quad (9)$$

where $l = 1..2^N-2$. To avoid using three different cases it is useful to define two „virtual" transition levels of the ADC: $T[0] = -\infty$ and $T[2^N] = +\infty$. This way the value of $Y(k)$ can be expressed in using (9) where now $l = 0..2^N-1$. The likelihood function of the measurement is

$$L(\mathbf{p})=\prod_{k=1}^{M}\mathrm{P}\left[Y(k)=y(k)\right] \quad (10)$$

where $y(k)$ is the k[th] sample of the digital record. Merging the equations above, one can express the likelihood function this way:

$$L(\mathbf{p})=\prod_{k=1}^{M}\frac{1}{2}\left[\operatorname{erf}\left(\frac{T[l+1]-x(t_k)}{\sigma\sqrt{2}}\right)+\operatorname{erf}\left(\frac{T[l]-x(t_k)}{\sigma\sqrt{2}}\right)\right] \quad (11)$$

For computations it is feasible to define a cost function, which is the negative log-likelihood function:

$$\mathrm{CF}(\mathbf{p})=-\ln L(\mathbf{p})=M*\ln(2)-\sum_{k=1}^{M}\ln\left[\operatorname{erf}\left(\frac{T[l+1]-x(t_k)}{\sigma\sqrt{2}}\right)+\operatorname{erf}\left(\frac{T[l]-x(t_k)}{\sigma\sqrt{2}}\right)\right] \quad (12)$$

3 First order derivatives of the cost function

To ease the expression of the formulas, let us use the following notation. Let arg(k) denote the argument of the natural logarithm function in the k[th] element of the cost function. This means that arg(k) is two times larger than the probability of measuring $y(k)$ for the k[th] sample, assuming parameters **p**.

$$\arg(k)=\operatorname{erf}\left(\frac{T[l+1]-x(t_k)}{\sigma\sqrt{2}}\right)+\operatorname{erf}\left(\frac{T[l]-x(t_k)}{\sigma\sqrt{2}}\right) \quad (13)$$

The first order partial derivatives of the cost function are expressed below:

$$\frac{\partial CF}{\partial A}=-\sum_{k=1}^{M}\frac{1}{\arg(k)}*\frac{2}{\sqrt{\pi}}\left(e^{-\left(\frac{T[y(k)]-x(k)}{\sqrt{2}\sigma}\right)^2}-e^{-\left(\frac{T[y(k)+1]-x(k)}{\sqrt{2}\sigma}\right)^2}\right)*\frac{\cos(k\theta)}{\sqrt{2}\sigma} \quad (14)$$

$$\frac{\partial CF}{\partial B}=-\sum_{k=1}^{M}\frac{1}{\arg(k)}*\frac{2}{\sqrt{\pi}}\left(e^{-\left(\frac{T[y(k)]-x(k)}{\sqrt{2}\sigma}\right)^2}-e^{-\left(\frac{T[y(k)+1]-x(k)}{\sqrt{2}\sigma}\right)^2}\right)*\frac{\sin(k\theta)}{\sqrt{2}\sigma} \quad (15)$$

$$\frac{\partial CF}{\partial C}=-\sum_{k=1}^{M}\frac{1}{\arg(k)}*\frac{2}{\sqrt{\pi}}\left(e^{-\left(\frac{T[y(k)]-x(k)}{\sqrt{2}\sigma}\right)^2}-e^{-\left(\frac{T[y(k)+1]-x(k)}{\sqrt{2}\sigma}\right)^2}\right)*\frac{1}{\sqrt{2}\sigma} \quad (16)$$

$$\frac{\partial CF}{\partial \theta}=-\sum_{k=1}^{M}\frac{1}{\arg(k)}*\frac{\partial\arg(k)}{\partial\theta} \quad (17)$$

where

$$\frac{\partial\arg(k)}{\partial\theta}=-\frac{2}{\sqrt{\pi}}\left(e^{-\left(\frac{T[y(k)]-x(k)}{\sqrt{2}\sigma}\right)^2}-e^{-\left(\frac{T[y(k)+1]-x(k)}{\sqrt{2}\sigma}\right)^2}\right)*\frac{A\sin(k\theta)k-B\cos(k\theta)k}{\sqrt{2}\sigma} \quad (18)$$

$$\frac{\partial CF}{\partial \sigma}=-\sum_{k=1}^{M}\frac{1}{\arg(k)}*\frac{\partial\arg(k)}{\partial\sigma} \quad (19)$$

where

$$\frac{\partial\arg(k)}{\partial\sigma}=-\frac{2}{\sqrt{\pi}}\left(e^{-\left(\frac{T[y(k)]-x(k)}{\sqrt{2}\sigma}\right)^2}*\frac{T[y(k)]-x[k]}{\sqrt{2}\sigma^2}-e^{-\left(\frac{T[y(k)+1]-x(k)}{\sqrt{2}\sigma}\right)^2}*\frac{T[y(k)+1]-x[k]}{\sqrt{2}\sigma^2}\right) \quad (20)$$

The partial derivatives with respect to the code transition levels are the following:

$$\frac{\partial CF}{\partial T[l]}=-\sum_{k=1}^{M}\frac{1}{\arg(k)}*\frac{\partial\arg(k)}{\partial T[l]} \quad (21)$$

where

$$\frac{\partial\arg(k)}{\partial T[l]}=\begin{cases}\frac{2}{\sqrt{\pi}}*e^{-\left(\frac{T[l]-x(k)}{\sqrt{2}\sigma}\right)^2}*\frac{T[l]-x(k)}{\sigma^2}, & y(k)=l-1\\ \frac{-2}{\sqrt{\pi}}*e^{-\left(\frac{T[l]-x(k)}{\sqrt{2}\sigma}\right)^2}*\frac{T[l]-x(k)}{\sigma^2}, & y(k)=l\\ 0, \text{ otherwise}\end{cases} \quad (22)$$

4 The Fisher Information

The Fisher information [4] matrix of a measurement record, assuming parameter vector **p** is the following:

$$I(\mathbf{p})_{i,j}=-E\left\{\frac{\partial^2\ln(L(\mathbf{p}))}{\partial p_i\partial p_j}\right\}=E\left\{\frac{\partial^2\mathrm{CF}(\mathbf{p})}{\partial p_i\partial p_j}\right\} \quad (23)$$

This means that the elements of the Fisher information matrix can be expressed as the expected values of the second order derivatives of the cost function defined previously. This

way the Hessian matrix of the cost function shall be expressed - which is also useful while it is evaluated during the numerical optimization of the cost function. Note that the expression of the cost function CF(**p**) does not use any random variables. The elements of the measurement record ($y(k)$, k = 1..M) are not random variables either. This way the value of CF(**p**) is deterministic and the values of its higher order derivatives are deterministic as well. Hence we can calculate the elements of the Fisher information matrix directly:

$$I(\mathbf{p})_{i,j} = E\left\{\frac{\partial^2 \mathrm{CF}(\mathbf{p})}{\partial p_i \partial p_j}\right\} = \frac{\partial^2 \mathrm{CF}(\mathbf{p})}{\partial p_i \partial p_j} \tag{24}$$

The general form of the elements of the Fisher information matrix is the following:

$$I(p)_{i,j} = \sum_{k=1}^{M} \frac{1}{\arg^2(k)} * \frac{\partial \arg(k)}{\partial p_i} * \frac{\partial \arg(k)}{\partial p_j} - \sum_{k=1}^{M} \frac{1}{\arg(k)} * \frac{\partial^2 \arg(k)}{\partial p_i \partial p_j} \tag{25}$$

Owing to the large amount of formulas this paper does not itemize all the elements of the Fisher information matrix, only shows an interesting part of them. The entire description of the Fisher information matrix is available in [4]. The second order derivatives with respect to the code transition levels deserve attention. The l+5th row and the l+5th row of the Fisher information matrix contains the following element:

$$\frac{\partial^2 CF}{\partial T[m] \partial T[l]} = * \frac{\partial \arg(k)}{T[l]} - \sum_{k=1}^{M} \frac{1}{\arg(k)} * \frac{\partial^2 \arg(k)}{\partial T[m] \partial T[l]} \tag{26}$$

where

$$\frac{\partial^2 \arg(k)}{\partial T[m] \partial T[l]} = f(x) = \begin{cases} \dfrac{\partial^2 \arg(k)}{\partial T[l]^2}, & l = m \\ 0, & \text{otherwise} \end{cases} \tag{27}$$

where

$$\frac{\partial^2 \arg(k)}{\partial T[l]^2} = \begin{cases} \dfrac{2}{\sqrt{\pi}} * e^{-Q_u^2(k)} * \dfrac{1}{\sigma^2} * \left(2Q_u(k) - 1\right), & y(k) = l - 1 \\ \dfrac{-2}{\sqrt{\pi}} * e^{-Q_l^2(k)} * \dfrac{1}{\sigma^2} * \left(2Q_l(k) - 1\right), & y(k) = l \\ 0, & \text{otherwise} \end{cases} \tag{28}$$

where

$$Q_u(k) = \frac{T\left[y(k)+1\right] - x(k)}{\sqrt{2}\sigma} \quad \text{and} \quad Q_l(k) = \frac{T\left[y(k)\right] - x(k)}{\sqrt{2}\sigma} \tag{29}$$

The first sum in (26) is nonzero if and only if $m = l$ or $m = l$ -1 or $m = l + 1$. The second sum in that equation is nonzero if and only if $m = l$. This way the (6..2^N+4,6..2^N+4) minor of the Fisher information matrix is tridiagonal. This fact will ease to calculate the inverse of the Fisher information matrix, which is the Cramér-Rao Lower Bound of the parameter estimators. The inversion of the Fisher information matrix raises two main challenges. The numerical condition of the matrix can be poor: the sensitivity to the frequency estimator can be larger than the other sensitivities by several orders of magnitude. In this case the adjustment of frequency scaling can be the solution as described in [6]. The other source of numerical problems is when some code transition levels do not appear in the likelihood function. This can happen if none of the adjacent code bins of the transition levels has been hit during the excitation. In this case the rows and the columns of the Fisher information matrix corresponding to these transition levels contain zeros. To solve the problem, we have to remove these parameters from the model (since they do not affect the measurement) and calculate the adequate minor of the Fisher information matrix. This minor matrix can be inverted and one can get the proper CRLB. Naturally this CRLB will not contain any information regarding the neglected code transition levels.

5 Comparison of Cramér-Rao Lower Bounds

The Cramér-Rao Lower Bounds [7] for estimation of sine wave parameters have been expressed for less complex models, these formulas appear in the literature. In Subsections 5.1 and 5.2 the CRLB of the frequency and amplitude estimation will be compared to results published previously.

5.1 Cramér-Rao Lower Bound for amplitude estimation

The expression of the CRLB for amplitude estimation appears in [8] based on [10]. For the estimator of the amplitude of the k^{th} harmonic component (R_k) the theoretical lower bound of the variance is

$$CRLB\left(\sigma_{R_k}^2\right) \cong \frac{2\sigma_n^2}{M} \tag{30}$$

where σ_n denotes the standard deviation of the additive noise on the multiharmonic signal and M denotes the number of recorded samples. In our signal model the sine wave is decomposed to a cosine component (coefficient A) and a sine component (coefficient B). This way the amplitude of the signal (R) can be described as

$$R = \sqrt{A^2 + B^2} \tag{31}$$

Hence

$$\mathrm{var}\left(\hat{R}\right) = c_A^2 * \mathrm{var}\left(\hat{A}\right) + c_B^2 * \mathrm{var}\left(\hat{B}\right) \tag{32}$$

where

$$c_A = \frac{\partial R}{\partial A} = \frac{A}{\sqrt{A^2 + B^2}} = \frac{A}{R} \quad \text{and} \quad C_B = \frac{\partial R}{\partial B} = \frac{B}{\sqrt{A^2 + B^2}} = \frac{B}{R} \tag{33}$$

This also means

$$\mathrm{CRLB}\left(\sigma_{R_k}^2\right) = \left(\frac{A}{R}\right)^2 * \mathrm{CRLB}\left(\sigma_A^2\right) + \left(\frac{B}{R}\right)^2 * \mathrm{CRLB}\left(\sigma_B^2\right) \tag{34}$$

The comparison has been performed using the parameters described in Subsection 6.1, but the number of samples covers a wider range, it increases from 10^4 up to 10^7. The results appear in Fig. 1. The blue stars show the CRLB calculated using the additive noise model and the red points show the CRLB calculated using the quantizer model and the Fisher information as described in the previous sections.

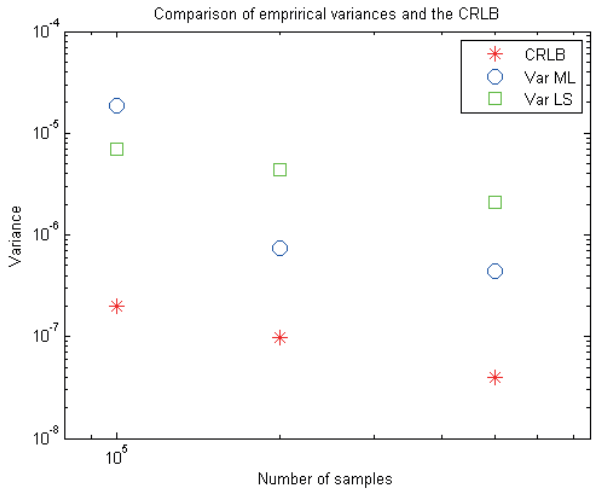

Fig. 1 Comparison of CRLBs of amplitude estimators

The log-log scale of Fig. 1 shows that the CRLB is inversely proportional to M in both cases, however the CRLB using the quantizer model is always lower than the CRLB using the additive noise model. The ratio is in the range of [63.72%..64.07%].

5.2 Cramér-Rao Lower Bound for frequency estimation

The expression of the CLRB for the estimation of the fractional period of a sampled sine wave appears in [9] based on [10]. In this paper the fractional period has been expressed the following way:

$$\frac{f}{f_s} = \frac{l+\delta}{M} \tag{35}$$

Where l is the integer part and δ is the fractional part of the number of periods. In this approach the frequency estimation task is to estimate the fractional period δ. The variance of estimator $\hat{\delta}$ has a theoretical lower bound. According to [9]

$$CRLB\left(\sigma_\delta^2\right) \cong \frac{6}{\pi^2} * \frac{\sigma_n^2}{A^2 M} \tag{36}$$

where σ_n is the standard deviation of the additive noise on the sine wave, A is the amplitude of the sine wave and M is the number of samples. Note the attractive properties of this expression: the CRLB is directly proportional to the variance of the additive noise and inversely proportional to the power of the sine wave (thus inversely proportional to the signal-to-noise ratio). Furthermore it is inversely proportional to the number of samples such as the variance of the mean of independent observations. The approximation sign in (36) is owing to a first-order Taylor approximation in a variance calculation: the variance of a spectral quantity has been approximated by the variances of its components weighted by its squared sensitivity to these components (see [9] and [10]). Since our signal model uses parameter $\theta = 2\pi f / f_s$ it is advantageous to express this CRLB in the terms of θ.

$$\theta = 2\pi \frac{l+\delta}{M} = \frac{2\pi l}{M} + \frac{2\pi\delta}{M} \tag{37}$$

Since the integer part of the periods (l) is constant in case of minor changes in frequency

$$\mathrm{var}\{\theta\} = \mathrm{var}\left\{\frac{2\pi\delta}{M}\right\} = \frac{(2\pi)^2}{M^2} * \mathrm{var}\{\delta\} \tag{38}$$

This way

$$CRLB\left(\sigma_\theta^2\right) = \frac{(2\pi)^2}{M^2} * CRLB\left(\sigma_\delta^2\right) = \frac{24\sigma_n^2}{A^2 * M^3} \tag{39}$$

The comparison has been performed using the parameters described in Subsection 6.1 but the number of samples covers a wider range, it increases from 10^4 up to 10^7. The results appear in Fig. 2. The blue stars show the CRLB calculated using the additive noise model and the red stars show the CRLB calculated using the quantizer model and the Fisher information as described in the previous sections.

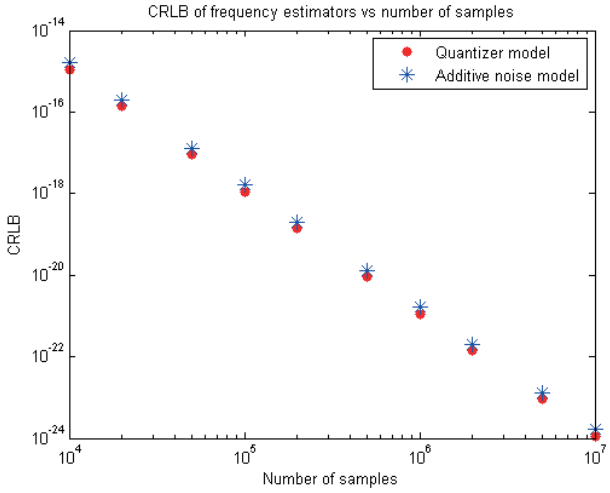

Fig. 2 Comparison of CRLBs of frequency estimators

The log-log scale of Fig. 2 shows that the CRLB is proportional to M^{-3} in both cases, however the CRLB using the quantizer model is always lower than the CRLB using the additive noise model. The ratio is in the range of [68.90%..69.34%].

6 Comparison of the empirical covariance of estimator populations with the Cramér-Rao Lower Bound

The theoretical lower bound of the covariance is important to evaluate the measurement results correctly and to design the measurement to fit for purpose. Considering the theoretical limits one can avoid to make decisions based on estimation results within the error margin and can also set measurement parameters to achieve variance and bias low enough to get useful estimators. In the following subsections empirical covariance of estimator populations achieved via simulated and real measurements are compared to the CRLB of covariance. Naturally not all the parameters are examined in this paper, only the investigation results of the most important ones are itemized in Subsections 6.1 and 6.2.

6.1 Estimator populations from simulated measurements

For the simulated measurements the parameter set was the following:

- **Quantizer:** 8-bit nonideal quantizer, INL_{max} = 2 LSB
- **Excitation signal:** 97 periods of sine wave, amplitude = 120% Full Scale, THD = -70dB, additive Gaussian white noise σ = 1 LSB.
- **Number of samples:** 10k, 20k, 100k, 200k, 500k, 1M, 2M
- **Number of simulated records with the same parameter set**: 50

For each number of samples a set of 50 different simulated measurement records have been generated. The 50 records have the same parameters, the same amount of noise but the noise realization is different from record to record. The statistics are generated from the populations of the 50 different estimators of the same parameter. The simulated measurement records are available at [11]. For each population and estimator type the following quantities have been calculated:

- Empirical variance of the estimator using 4-parameter least squares fit as described in [11] and [12].
- Empirical variance of the estimator using ML estimation of the parameter
- Cramér-Rao Lower Bound for the variance of the estimator as described in Section 4

These quantities are shown in Fig. 3 and Fig. 4.

6.1.1 Results for frequency estimators

As Fig. 3 shows the variance of the LS frequency estimators is lower than the variance of the ML estimators for the lower number of samples. This can be explained by the relatively low number of samples in a code bin. In these cases the large uncertainty of code transition level estimators affects the uncertainty of other parameter estimators, this way the LS estimators perform better for lower numbers of samples. Above 10^5 samples the variance of the ML estimators becomes the lower one.

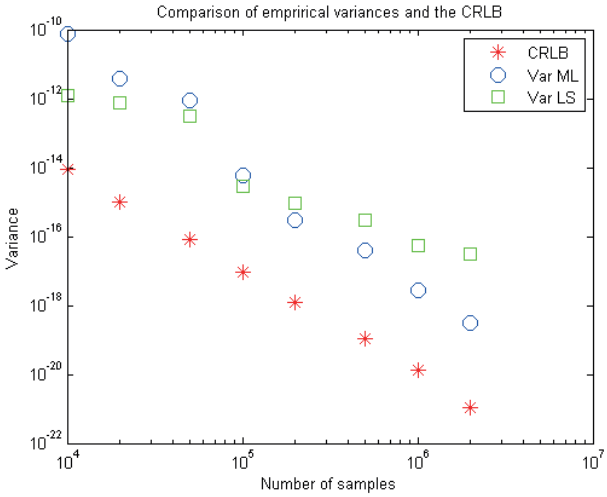

Fig. 3 Empirical variance of frequency estimators and the CRLB (simulated measurements)

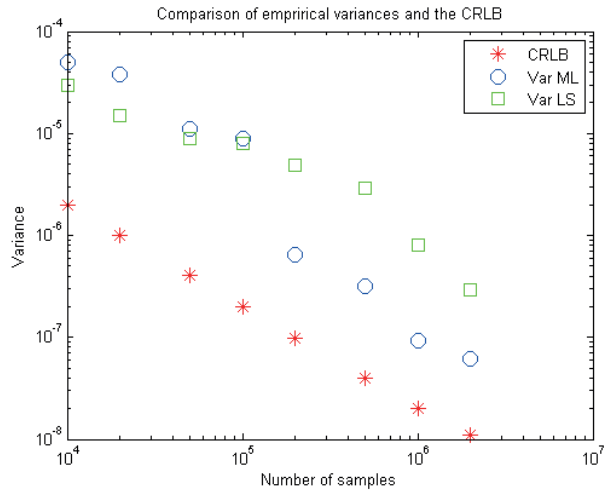

Fig. 4 Empirical variance of amplitude estimators and the CRLB (simulated measurements)

6.1.2 Results for amplitude estimators

The tendencies in Fig. 4 are largely similar to the tendencies of the frequency estimators. The empirical variance of the LS estimators is lower than the variance of the ML estimators for relatively low numbers of samples, however at larger number of samples the asymptotically efficient property of ML estimators shows itself and the variance of the ML estimators becomes significantly lower than the variance of the LS estimators. The empirical variance of the ML estimators does not reach the CRLB for these finite numbers of samples, but ML estimators show more attractive asymptotic behaviour than LS estimators do.

6.2 Estimator populations from real measurements

The measurements were designed to be largely similar to the simulations itemized in Section 6.1. The sine wave generator was a Bruel & Kjaer 1051 device, the ADC under test was the ADC of an NI-9201 data acquisition board. Since the

resolution of this SAR ADC is 12 bits, the codes have been truncated to the 8 most significant bits. Discarding the 4 least significant bits we gained an 8-bit SAR quantizer with low INL values. The frequency of the sine wave was set to 97 Hz, the time duration of the measurement was 1 second, and the sampling rate was 100 kHz, 200 kHz and 500 kHz. This way the number of acquired samples in a record was 100k, 200k and 500k. For each measurement setup 50 different measurements have been performed. The measurements have been automated using the NI LabWIEW environment. To ensure identical initial phase of the sine wave for the corresponding measurements is a difficult task in this case. However, it can be solved scheduling the automated measurements synchronized to the period of the excitation sine wave.

6.2.1 Results for frequency estimators

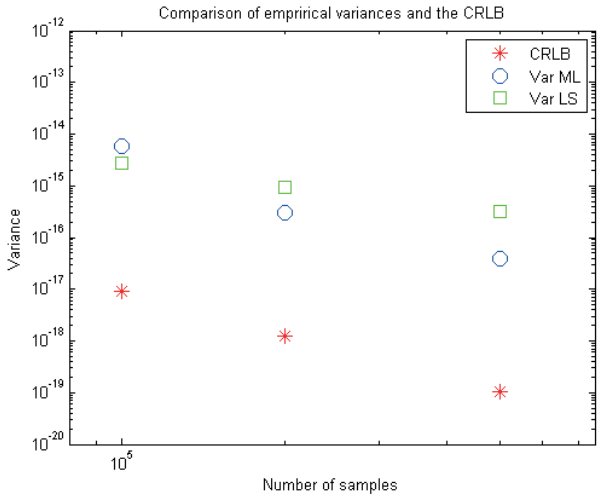

Fig. 5 Empirical variance of frequency estimators and the CRLB (real measurements)

6.2.2 Results for amplitude estimators

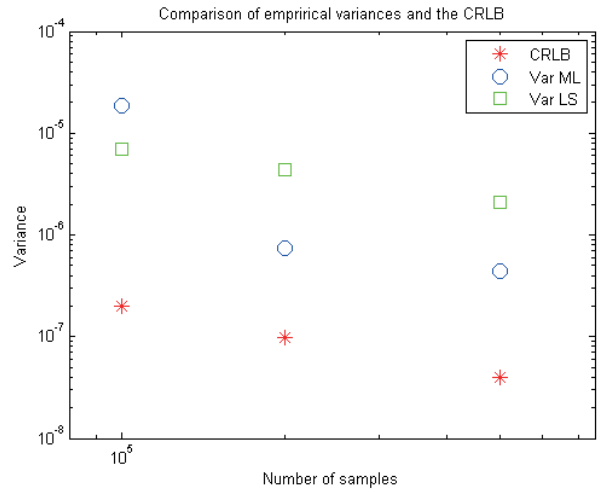

Fig. 6 Empirical variance of amplitude estimators and the CRLB (real measurements)

The variance of amplitude estimators has been calculated using the method that is described in Subsection 5.1. The results of the measurement evaluation appear in Fig. 5 and Fig. 6. These figures show the same quantities as Fig. 3 and Fig. 4 do – empirical covariance of the ML and LS estimators and the calculated value of the CRLB -, but the real measurements were performed using only three different numbers of samples. The results achieved via real measurements are largely similar to the results detailed in Subsection 6.1. The largest difference between the variances calculated based on simulated and real measurements was 57.16% which is acceptable considering that the variance values cover multiple orders of magnitudes in this case. A conclusion can be drawn up for both amplitude and frequency estimators and for both simulated and real measurements: the variance of the ML estimators is higher than the LS ones for lower number of samples, but the relation changes to its opposite for higher number of samples. Since ML estimators are efficient, this observation fits to the theory regarding the asymptotical properties of ML estimators.

7 Generalization for arbitrary band-limited periodic signals

The signal model introduced in Section 2 assumes a pure sine wave with Gaussian additional noise but without harmonic distortion. However, handling upper harmonic components does not raise invincible challenges, only scales up the size of the parameter space. Assuming a band-limited periodic excitation, our signal model is the following:

$$x(t)=\sum_{i=1}^{L}A_i\cos(2\pi ift)+\sum_{i=1}^{L}B_i\sin(2\pi ift)+C \qquad (40)$$

where L is the number of harmonic components (including the fundamental harmonic). The parameter vector in this case is the following:

$$\mathbf{p}^T=\left[A_1\ldots A_L\,B_1\ldots B_L\,C\,\theta\,\sigma\,T[1]\ldots T\left[2^N-1\right]\right] \qquad (41)$$

The partial derivatives with respect to A_i and B_i can be calculated easily using the derivatives with respect to A and B from the original (pure sine wave) signal model, e. g.

$$\frac{\partial\arg(k)}{\partial A_i}=\frac{2}{\sqrt{\pi}}\left(e^{-\left(\frac{T\lfloor y(k)\rfloor-x(k)}{\sqrt{2}\sigma}\right)^2}-e^{-\left(\frac{T\lfloor y(k)+1\rfloor-x(k)}{\sqrt{2}\sigma}\right)^2}\right)\frac{\cos(ki\theta)}{\sqrt{2}\sigma} \qquad (42)$$

or

$$\frac{\partial\arg(k)}{\partial B_i}=\frac{2}{\sqrt{\pi}}\left(e^{-\left(\frac{T\lfloor y(k)\rfloor-x(k)}{\sqrt{2}\sigma}\right)^2}-e^{-\left(\frac{T\lfloor y(k)+1\rfloor-x(k)}{\sqrt{2}\sigma}\right)^2}\right)\frac{\sin(ki\theta)}{\sqrt{2}\sigma} \qquad (43)$$

Concerning second order and mixed second order derivatives with respect to A_i and B_i these can be calculated using the derivatives w. r. t. A and B using the following substitutions:

- $\cos(k\theta) \to \cos(ki\theta); \sin(k\theta) \to \sin(ki\theta)$
- $\cos(k\theta)k \to \cos(ki\theta)ki; \sin(k\theta k) \to \sin(ki\theta)ki$
- $\cos(k\theta)k^2 \to \cos(ki\theta)k^2i^2; \sin(k\theta)k^2 \to \sin(ki\theta)k^2i^2$

Using this extension of the signal model the problem of estimating signal and quantizer parameters simultaneously from the same measurement record can be solved for all those cases when the excitation is a band-limited periodic signal. This can be advantageous from two reasons.

- This way we can handle those cases where the excitation signal contains higher harmonics *intentionally* e.g. where the excitation is a multisine wave.
- Using this extension we can also handle those cases where the harmonic distortion of the excitation sine wave is large enough to mislead the sine wave fitting and thus the qualification of the quantizer. If the harmonic distortion of the excitation signal is not estimated and the perceived harmonic distortion is assigned to the quantizer than the quantizer will be seemingly worse than its real quality.

8 Conclusions

The calculations, the simulation and measurement results detailed in this paper provide the following main conclusions:

- The Fisher Information matrix and the Cramér-Rao Lower Bound can be calculated for maximum likelihood estimation of quantizer and sine wave parameters. The numerical condition of the Fisher Information matrix can raise challenges; however these challenges can be answered.
- The CRLB of the ML model has been compared to the CRLB of a less complex model. This comparison shows that the asymptotic properties of these CRLBs are largely similar, however the CRLB based on a more complex model is lower than the CRLB of the simple additive noise model.
- The empirical variance of the ML estimators has been compared to the empirical variance of the LS estimators based on simulated and real measurements. These variances have also been compared to the corresponding CRLBs.
- The signal model has been extended from noisy sine wave to an arbitrary noisy bandlimited periodic signal. Section 7 showed that this extension only increases the scale of the problem, but does not increase its theoretical complexity.

The experiments detailed in this paper can be reproduced, modified and extended using the open source ADCTest toolbox for MATLAB [4], the raw data (simulated and real measurement records) are available at [13].

Acknowledgement

This work has been supported by the National Research, Development and Innovation Office (NKFIH) Grant No. K115820.

References

[1] Dudley, R. M. "*Real Analysis and Probability*." Cambridge Studies in Advanced Mathematics (No. 74.), Cambridge University Press, Cambridge. 2010. https://doi.org/10.1017/CBO9780511755347

[2] Pálfi, V., Virosztek, T., Kollár, I. "Full information ADC test procedures using sinusoidal excitation, implemented in MATLAB and LabVIEW." *ACTA IMEKO*. 4(3), pp. 4-13. 2015. URL: https://acta.imeko.org/index.php/acta-imeko/article/viewFile/IMEKO-ACTA-04%20(2015)-03-02/427

[3] Balogh, L., Kollar, I., Sárhegyi, A. "Maximum likelihood estimation of ADC parameters." In: I2MTC 2010 - IEEE International Instrumentetion and Measurement Conference, Austin, Texas, USA, May 3-6, 2010. https://doi.org/10.1109/IMTC.2010.5488286

[4] Fisher, R. A. "Theory of statistical estimation." *Mathematical Proceedings of the Cambridge Philosophical Society*. 22(5), pp. 700-725. 1925. https://doi.org/10.1017/S0305004100009580

[5] ADCTest toolbox - Users' guide. Version 4.4. URL: http://www.mit.bme.hu/projects/adctest

[6] Renczes, B., Kollár, I., Moschitta, A., Carbone, P. "Numerical Optimization Problems of Sine-Wave Fitting Algorithms in the Presence of Roundoff Errors." *IEEE Transactions on Instrumentation and Measurement*. 65(8), pp. 1785-1795. 2016. https://doi.org/10.1109/TIM.2016.2562218

[7] Radakrishna Rao, C. "Information and the accuracy attainable in the estimation of statistical parameters. *Bulletin of the Calcutta Mathematical Society*. 37(3), pp. 81–91. 1945.

[8] Belega, D., Dallet, D., Slepička, D. "Accurate Amplitude Estimation of Harmonic Components of Incoherently Sampled Signals in the Frequency Domain." *IEEE Transactions on Instrumentation and Measurement.* 59(5), pp. 1158-1166. 2010. https://doi.org/10.1109/TIM.2010.2045144

[9] Belega, D., Dallet, D., Petri, D. "Accuracy of the Normalized Frequency Estimation of a Discrete-Time Sine-Wave by the Energy-Based Method." *IEEE Transactions on Instrumentation and Measurement*. 61(1), pp. 111-121. 2012. https://doi.org/10.1109/TIM.2011.2159318

[10] Offelli, C., Petri, D. "The Influence of Windowing on the Accuracy of Multifrequency Signal Parameter Estimation." *IEEE Transactions on Instrumentation and Measurement.* 41(2), pp. 256-261. 1992. https://doi.org/10.1109/19.137357

[11] IEEE Standard for Terminology and Test Methods for Analog-to-Digital Converters. IEEE-1241-2010. 14 Jan 2011. https://doi.org/10.1109/IEEESTD.2011.5692956

[12] IEEE Standard for Digitizing Waveform Recorders. IEEE-1241-2007. 18 April 2008. https://doi.org/10.1109/IEEESTD.2008.4494996

[13] Raw data for article PPEECS-2016-CRLB. http://home.mit.bme.hu/~virosztek/publicationdata/ppeecs-2016-crlb